LA-UR -86-2838

MASTER

Los Alamos National Laboratory is operated by the University of California for the United States Department of Energy under contract W-7405-ENG-36

CONF-861165--2

TITLE MODELING OF EXTERNAL RADIATION FROM THE TRANSPORT OF RADIONUCLIDES ACROSS A CANYON

LA-UR--86-2838

DE86 015298

AUTHOR(S): B. M. Bowen, HSE-8
W. A. Olsen, HSE-8
D. Van Etten, HSE-8
I-Li Chen, HSE-8

SUBMITTED TO: 5th Joint Conf. on Applications of Air Pollution Meteorology, Raleigh, NC
November 17-20, 1986

Los Alamos Los Alamos National Laboratory
Los Alamos, New Mexico 87545

FORM NO 836 R4
ST NO 2629 5/81

DISTRIBUTION OF THIS DOCUMENT IS UNLIMITED

MODELING OF EXTERNAL RADIATION FROM THE TRANSPORT OF RADIONUCLIDES ACROSS A CANYON

Brent M. Bowen, William A. Olsen, Donald Van Etten, and I-li Chen

Los Alamos National Laboratory
Los Alamos, New Mexico

1. INTRODUCTION

The Los Alamos Meson Physics Facility (LAMPF) is an 800-million electron volt, 1 mA intensity linear proton accelerator used for studying subatomic particles at relativistic velocities. Routine operation of the accelerator results in the formation of short-lived air activation products, primarily in the beam stop section of LAMPF.

Offsite radiation exposure levels from LAMPF operations have been routinely monitored in the location of maximum exposure since 1977 with a network of thermoluminescent dosimeters (TLDs). In 1982, a pressurized ionization chamber (PIC) was placed at the fenceline location of the maximum external radiation level (Bowen 1982). This instrument has the ability to monitor very low external radiation levels over short-time periods, and is used with the TLD measurements to estimate external radiation levels. Also, a Gaussian-type model, using onsite meteorological data and radionuclide release rates, is then used to predict daily radiation exposures and is compared with the PIC measurements.

This study presents the results of monitoring and modeling external radiation levels from LAMPF emissions at three locations during 1984. Measured radiation exposures are presented for all three locations during a 49-day period. Hourly radiation levels are calculated for all sites and compared with the prevalent wind patterns during the study period. Predicted daily levels are compared with measured values at all of the sites. Accuracy of the model is compared for day and night conditions. Annual model predictions are also compared with TLD measurements.

2. BACKGROUND

The Los Alamos National Laboratory is located on the Pajarito Plateau on the eastern flanks of the Jemez Mountains. The Sangre de Cristo Mountains lie nearly 70 km to the east. The Rio Grande Valley runs north-northeast to south-southwest between the two mountain ranges. The plateau slopes downward to the east from the base of the Jemez Mountains (approximately 2500 m above sea level or MSL) to the Rio Grande (approximately 1700 MSL) over a distance of 25 km. There also are numerous alternating "finger" mesas and canyons running along the slope line of the plateau. The canyons are 50-100 m deep and 100-200 m wide, while the mesas vary from 200-600 m in width. LAMPF is located on a mesa top just south of Los Alamos Canyon.

The LAMPF stack is located about 800 m south of the closest Laboratory boundary location across the Los Alamos Canyon. Three short-lived, gaseous radioactive air activation products, ^{15}O, ^{11}C, and ^{13}N, account for virtually all downwind radiation levels. Because of the annihilation of positrons from the decay of these radionuclides, 0.511 MeV photon radiation is emitted from the plume of gases as it travels downwind from the stack. However, the total amount of radiation in the plume decreases with time (or downwind distance) as the gases decay. Some characteristics of these three radioactive gases are shown in Table I. Note that most of the radioactivity released is ^{15}O. However, the half-life ($T^{1/2}$) of ^{15}O is only 123 s. The contribution of ^{15}O to the total radioactivity in the plume at the Laboratory boundary increases with increasing windspeed. Note that although much less ^{11}C is emitted than ^{15}O, more ^{11}C remains at the Laboratory boundary distance than ^{15}O for windspeeds under 3 m/s. For greater windspeeds, ^{15}O becomes the dominant gas. The contribution of ^{13}N to the total radioactivity is small because it comprises only a small percentage of the releases and has a relatively short half-life.

Table I shows that the total radioactivity in the plume varies greatly with the windspeed. At higher windspeeds, the reduced cross canyon travel time results in less radioactive decay; however, stronger windspeeds enhance dilution of the gases causing lower concentrations downwind. The "decay factor" of the radionuclide mixture mitigates much of the "dilution factor" with increasing windspeed. Therefore, over the typical windspeed range, photon radiation levels from the plume are expected to decrease slightly with increasing windspeed. Also, windspeed can affect the stability, and in turn, indirectly affect plume concentrations and resulting gamma radiation.

3. SITING AND INSTRUMENTATION

3.1 LAMPF Releases

The study area is shown in Fig. 1. The LAMPF stack is 30 m high and has a diameter at the top of 0.9 m. A Kanne-type air-ionization instrument is used to monitor the radioactive gases before entering the stack. A volume is recorded, which is correlated to the total radionuclide air concentrations in curies per cubic meter (Ci/m^3) in the stack gas. The percentage compositions of ^{15}O, ^{11}C, and ^{13}N in the stack gas have been determined previously by analyzing bag samples of the stack gas. Stack velocity is measured continuously by an anemometer placed halfway up the stack and by periodic stack tests.

Table I. Release Data of the Three Primary Radioactive Gases and Amounts of Radioactivity Remaining at 800 m Downwind

Radioactive Gases (%)	$T^{1/2}$ (s)	% Remaining at 800 m for Different Windspeeds			
		1 (m/s)	3 (m/s)	6 (m/s)	10 (m/s)
^{15}O (72)	123	1	22	47	64
^{11}C (16)	1230	64	86	93	96
^{13}N (4)	600	40	74	86	91
Total (92)	...	13	34	55	69

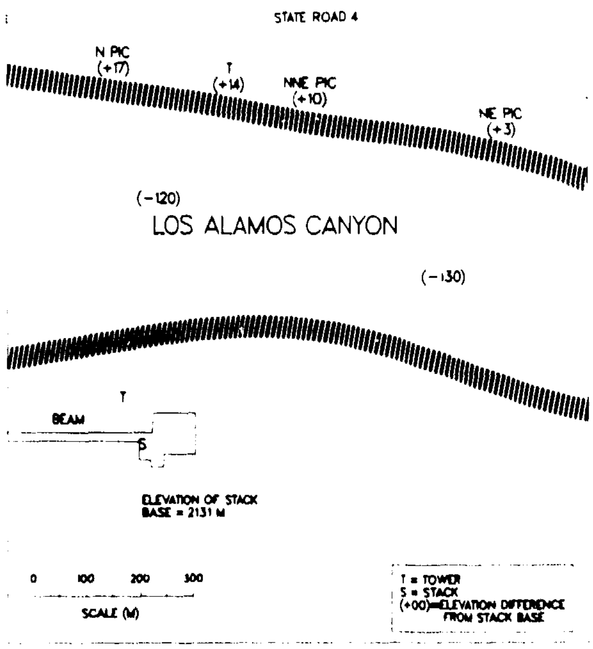

Fig. 1. Map of study area.

3.2 External Radiation Monitoring

Three PIC's monitored real-time photon exposures to air during 1984 at the nearest offsite boundary across the Los Alamos Canyon. The instruments were located at azimuths of 0° (north), 22° (north-northeast) and 45° (northeast) of the LAMPF stack. The PIC's located in the north and north-northeast are 725 m from the stack, while the northeast PIC is located 875 m from the stack. Each instrument uses a modified Reuter-Stokes high-pressure ionization chamber (Van Etten 1986). An array of 12 lithium fluoride TLD stations also monitors long-term gamma doses on a routine basis.

3.3 Meteorology

Meteorological data were collected for this study on a 12 m tower located between the north and north-northeast PIC's at a distance of 725 m and a bearing of 12° from the LAMPF stack (Fig. 1). Another tower is located about 100 m to the north-northwest of the stack on the LAMPF side of Los Alamos Canyon.

4. RESULTS AND DISCUSSION

4.1 Monitoring

The predominance of south-southwesterly and southwesterly winds at Los Alamos is illustrated by an hourly frequency diagram for the 49-day study period (Fig. 2). This period is representative of average annual winds. Note how an up-valley wind develops in the afternoon hours and becomes more frequent later in the evening and early morning hours. About 28% of all nighttime winds are southwesterly, while the directions south-southwest, southwest, and west-southwest account for a total of nearly 54% of nighttime winds. Much of the high frequency of southwesterly winds is probably caused by the channeling of the regional winds by the Rio Grande Valley. This process occurs more frequently at night when the vertical mixing is at a minimum.

By 0400 the frequency of up-valley winds decreases while down-valley winds become more important. By late morning, the

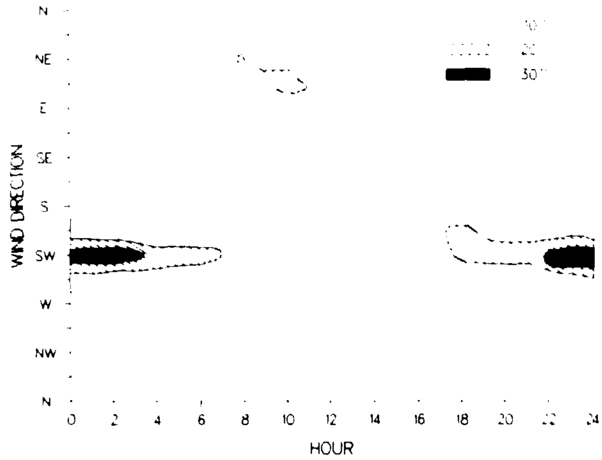

Fig. 2. Hourly frequency diagram of wind direction during a 49-day study period.

northeasterly winds, probably also caused by channeling, account for over 20% of all winds.

The daytime wind pattern is complex and varied. Besides the channeling effect, some southwesterly winds result from a mountain-valley wind up the Rio Grande Valley caused by strong solar heating (Bowen 1981). These winds are especially important during the summer season because of a lack of strong and persistent winds. An upslope wind also develops over the Plateau during the day at times of light large scale winds and strong sunshine. Note the occurrence of southeasterly and south-southeasterly winds during the late morning and afternoon hours.

The complex pattern of winds causes large variations of gamma levels* with time of day. Average hourly gamma levels caused by LAMPF emissions for the 49-day study period are shown in Fig. 3. Both the highest and lowest hourly averages occur at the northeast PIC. The highest averages of 40 μR/h occur around midnight because of the high frequency of southwesterly winds. Midday values are very low at the northeast site from a scarcity of up-valley winds at this time. The north-northeast site shows a similar, but more moderate daily gamma radiation variation. The north PIC shows a rather uniform average radiation level throughout the day. Increased daytime mixing of the atmosphere plays an important role in reducing gamma radiation levels at all three sites.

The increased daytime mixing is shown vividly in Fig. 4, which contains histograms of standard deviation of horizontal wind (σ_θ) and vertical wind (σ_ϕ) by hour. Values of both σ_θ and σ_ϕ are more than twice as large during the early afternoon hours as they are during the late-night and early-morning hours. The diurnal variation of the two are quite similar.

The variation during the day in the LAMPF release rate also contributes somewhat to radiation variations. Average hourly release rates for the study period were 10-20% lower during the day when routine maintenance of the LAMPF beam is the greatest.

4.2 Modeling

4.2.1 Discussion

Two major considerations in the modeling of radiation caused by a plume are the distance of the receptor from the plume and the intensity of the radiation emanating from it. These considerations are in addition to the problem of estimating the down-

---

*Exposure to air is expressed in units of roentgens. All gamma exposures, both measured and modeled, will be expressed in roentgens throughout this report. However, the units of roentgens and rems, the units of dose, are virtually interchangeable (1 R = 0.96 rem).

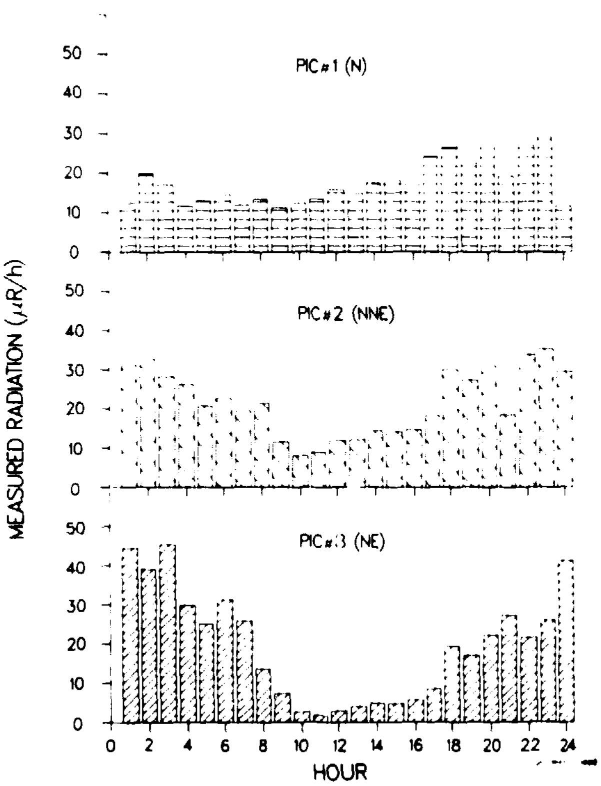

Fig. 3. Average hourly external radiation at three sites from LAMPF emissions during a 49-day study period.

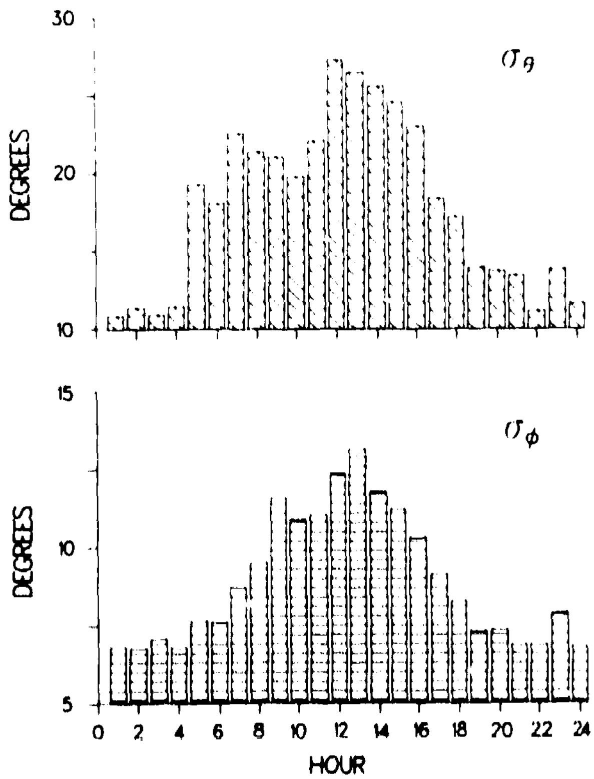

Fig. 4. Average hourly standard deviation of horizontal wind direction (σ_θ) and vertical wind (σ_ϕ) at East Gate during a 49-day study period.

wind configuration of the plume and the concentration of radionuclides within it. A gamma-emitting cloud with small dimensions compared with the distance the radiation travels is termed a finite cloud for modeling purposes. A method for calculating the exposure from a finite cloud has been developed by Healy (1968). This model contains integrals that account for the geometry of the passing plume with respect to the receptor. A considerable amount of computer time is required to calculate the integrals. Healy suggests using the finite cloud model when the standard deviation of the spread of the plume (σ) is less than 100 m or so.

A much simpler infinite cloud model can be used for gamma-ray plumes at relatively large downwind distances. The following model for infinite clouds is taken from *Meteorology and Atomic Energy* (Healy, 1968):

$$\gamma D = 0.457\ \bar{E}_\gamma \chi \quad , \tag{1}$$

where γD is the dose (rads) or exposure (roentgens), $\bar{E}_\gamma$ is the average gamma energy emitted at each disintegration (MeV/dis), and χ is the radionuclide concentration (curies/m^3). This equation can be used during equilibrium or near-equilibrium conditions when just as much energy-absorption per unit volume occurs as energy-release per unit volume. The value of γD is directly proportional to χ. Since χ is relatively easy to determine by using the Gaussian dispersion model, the infinite model is much easier to calculate than the finite model.

The finite model was used to predict 24-h exposures at the three sites by adding up 15-min estimates. The results indicated that the model underestimated the actual exposures by more than 50%.

The infinite model was then used to estimate 24-h gamma exposures at the three sites. Healy suggests that Eq. (1) be reduced by a factor of 0.5 for calculating ground level doses, because a receptor at the ground would only receive radiation from half the idealized cloud or plume. However, an empirically derived reduction factor of 0.25 was used instead.

The ground-level form of the Gaussian dispersion model was used to calculate χ. For long-term integrated concentrations, the seasonal sector averaged form of the Gaussian dispersion model was used. The dispersion coefficients σ_y and σ_z were determined directly from the onsite meteorological data using a method suggested by Draxler (1976). The stack release gas at LAMPF is very close to the ambient temperature. The stack rise is, therefore, expected to be from momentum only. The stack rise equation suggested by Briggs (1969) was used.

The different heights of the three receptors relative to the source were accounted for in the modeling. As a compromise, the plume was assumed for modeling purposes to travel halfway between constant terrain (mesa top) height and height above sea level. For example, the north PIC is at a height 17 m above the base of the LAMPF stack. For modeling purposes, this reduces to 8.5 m. Even at the north PIC, the highest monitor, this one-half height adjustment in the model only increases estimates approximately 10% over the case without height adjustment. The effect is even less at the north-northeast PIC, which is only 10 m higher than the ground level at LAMPF.

For simplicity, it is also assumed that all available gases in the plume cross the canyon. Realistically, some of the gases are lost by turbulence into the canyon. However, the transport of the radionuclides into the canyon by turbulent exchange is expected to be small compared with the amount transported across the canyon.

4.2.2 Daily Model Results

Daily model predictions, based on integration of 15-min predictions, were made and compared with measured values. Comparison of the predicted and measured values for the three sites are shown in Fig. 5. There is good correlation between the predicted and measured data. Correlation is strongest at the north-northeast site and weakest at the northeast site. However, even at the northeast site, the correlation coefficient is high at 0.83 with a corresponding r^2 value of 0.69. This implies that 69% of the variation of measured values is explained by the model at the

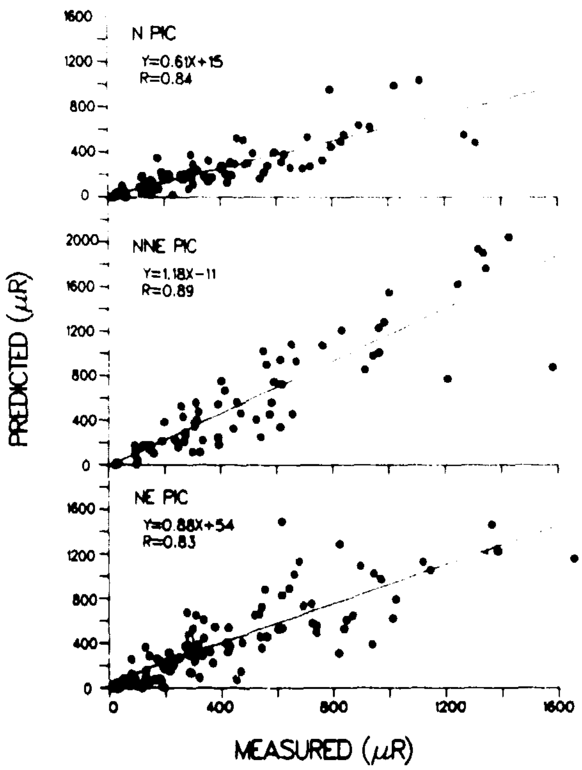

Fig. 5. Predicted versus measured daily external radiation from LAMPF emissions at sites N, NNE, and NE of LAMPF on State Road 4.

northeast PIC, with higher r^2 values at the other two sites. All three correlations are significant at the 99.9% confidence level.

Note that the model closely predicted measured exposures at the north-northeast and northeast PICs with slopes of nearly one. However, the slope of 0.61 at the north PIC indicates that the model underpredicts at this site. This rather large difference in slope of the north PIC data may be related to the large difference of wind frequency in south and south-southwest winds. Radiation from the plume traveling toward the north-northeast PIC possibly affects the north site. Or, the indicated wind direction may be several degrees greater than the actual direction causing the model to underpredict at the north site.

Average hourly predicted and measured values were also compared with each other over the study period. Results indicate that the ratio of predicted versus measured values is greater during the day than at night. One possible reason is that some of the radionuclides may be mixing down into the canyon during the day. Another explanation is that the model underestimates dispersion during unstable periods and/or overestimates dispersion during stable periods.

4.2.3 Long-Term Model Results

The long-term Gaussian model was used to estimate exposures at the three sites for the 49-day study period. These estimates are compared with the estimates derived from adding up the separate 24-h estimates and with the measured data (Table II). Results show that the long-term model is very useful in predicting exposures, but not as accurate as the short-term model. The long-term model yields estimates rather close to those of the short-term model, with both substantially underpredicting in the north sector. However, the long-term model does overpredict in the northeast sector.

Long-term exposures were also calculated for 1984 at locations along State Road 4. The estimated exposures (mR) are: 75 in the northeast, 90 in the north-northeast, 39 in the north, and 28 in the north-northwest. This gives an average of 59 mR for the sector from north-northwest through northeast. This compares with the 44 mR as reported by the TLD network.

Table II. Long-Term External Radiation Estimates Based on a Long-Term Model, Short-Term Model and Measurement (mR) (over 49-day study)

PIC Site	Long-Term Model	Short-Term Model	Measured
N	10.9	12.6	20.7
NNE	27.9	27.6	25.5
NE	33.0	22.0	23.0
N thru NE	23.9	20.7	23.1

5. SUMMARY AND CONCLUSIONS

The primary conclusions of the study are:

(1) A persistent, locally produced up-valley wind is responsible for causing the maximum exposures to occur to the northeast and north-northeast of LAMPF.
(2) The channeling of large-scale winds, especially at night, is most likely responsible for the high frequency of up-valley winds.
(3) External radiation is generally considerably higher during the nighttime hours because of decreased atmospheric dispersion and, to a lesser degree, increased emission rates.
(4) Predicted daily exposures using the simple infinite cloud approximation correlate very well with measured exposures. The more complex finite cloud model gives estimates more than 50% less than measured values.
(5) The short-term model does underpredict exposures to the north of LAMPF, especially during the nighttime and/or times with weak atmospheric mixing. However, these periods coincide with the persistent southwesterly and south-southwesterly up-valley winds. Photon radiation from the adjacent plume may affect the north PIC and is not accounted for in the model. Another possibility is that the indicated wind direction may be several degrees greater than the actual direction causing the model to underpredict at the N site.
(6) Based on these modeling results, a Gaussian model is expected to accurately predict radioactive or nonradioactive levels up to several miles downwind if onsite meteorological and source data are available. However, further calibration of the models using some form of tracer would increase confidence in the use of the models.

REFERENCES

Bowen 1981: B. M. Bowen, J. M. Dewart, and F. G. Fernald, "A Study of the Nocturnal Drainage Flow Over a Sloping Plateau in North-Central New Mexico," Proceedings of Second Conference on Mountain Meteorology, November 9-12, 1981, pp. 225-232, Am. Met. Soc.

Bowen 1982: B. M. Bowen, T. E. Buhl, J. M. Dewart, W. R. Hansen, D. Talley, A. I. Chen, W. A. Olsen, and D. M. Van Etten, "Measurements and Modeling of Gamma Absorbed Doses Due to Releases from a Linear Proton Accelerator: Experimental Design and Preliminary Results," Proceedings of Fourth DOE Environmental Protection Information Meeting, December 7-9, 1982, pp. 447-456.

Briggs 1969: G. A. Briggs, "Plume Rise," Atomic Energy Commission Critical Review Series, TID 25075 (1969).

Van Etten 1986: D. M. Van Etten and W. A. Olsen, "Improvement of a Portable Pressurized Ionization Chamber with the Addition of a Microprocessor Datalogger," Los Alamos National Laboratory report (to be published)